The crystal structure of $Na(NH_4)Mo_3O_{10}\cdot H_2O$

Joel W. Reid,[1,a] James A. Kaduk,[2] and Jeremy A. Olson[3]
[1]*Canadian Light Source, 44 Innovation Boulevard, Saskatoon, SK S7N 2V3, Canada*
[2]*Illinois Institute of Technology, 3101 S. Dearborn St., Chicago 60616, Illinois*
[3]*Canadian Isotope Innovations Corp., 232-111 Research Drive, Saskatoon, SK S7N 3R2, Canada*

(Received 5 January 2017; accepted 26 March 2017)

The crystal structure of $Na(NH_4)Mo_3O_{10}\cdot H_2O$ has been solved by parallel tempering using the FOX software package with synchrotron powder diffraction data obtained from beamline 08B1-1 at the Canadian Light Source. Rietveld refinement, performed with the software package GSAS, yielded orthorhombic lattice parameters of $a = 13.549\,82(10)$, $b = 7.618\,50(6)$, and $c = 9.302\,74(7)$ Å ($Z = 4$, space group *Pnma*). The structure is composed of molybdate chains running parallel to the *b*-axis. The Rietveld refinement results were compared with density functional theory calculations performed with CRYSTAL14, and show excellent agreement with the calculated structure. © *2017 International Centre for Diffraction Data*. [doi:10.1017/S0885715617000380]

Key words: ammonium sodium trimolybdate hydrate, powder diffraction, structure solution, density functional theory

I. INTRODUCTION

Molybdenum (Mo) is an element with interesting and complicated chemistry that impacts on numerous scientific and technological fields. Mo is an essential trace element in living organisms, present in a wide variety of enzymes and cofactors critical for life (Garner, 1994; Schwarz *et al.*, 2009). Isotopically, the element is notable for having seven stable isotopes of relatively high (>5%) abundance (Anbar, 2004). Mo compounds in general (Green, 1994; Roggan and Limberg, 2006), and Mo oxides in particular (Chippendale and Cheetham, 1994; Sławiński *et al.*, 2016), are well known to exhibit unusual and varied crystal chemistry. Mo sees widespread usage in steel and corrosion resistant alloys (Lasheen *et al.*, 2015), catalysis (Haber, 1994; Zaman and Smith, 2012), and medical isotope production, where reactor produced ^{99}Mo is used to produce technetium-99m (^{99m}Tc), the most widely used radioisotope for medical imaging (Banerjee *et al.*, 2001).

^{99}Mo has historically been produced using nuclear reactors, but concerns with the use of HEU (highly enriched uranium) and supply insecurity because of production by only a small number of aging reactors have led to significant interest in alternative production routes (National Research Council, 2009; Van Noorden, 2013). This has necessitated development of complementary chemical processes for Mo recycling to make these alternative production routes viable (Tkac and Vandergrift, 2016). The compound characterized in this work was observed during development of Mo recycling processes for accelerator based production of ^{99}Mo. Based on the formula and lattice parameters, the phase appears to have been observed previously (Förster *et al.*, 1985) without a detailed description of the crystal structure.

II. EXPERIMENTAL

A specimen of Mo processing powder supplied by Canadian Isotope Innovation Corp. was mounted in a 0.5 mm ID Kapton capillary, which was sealed at both ends with adhesive.

Powder X-ray diffraction (PXRD) patterns were collected using a Canadian Macromolecular Crystallography Facility beamline (CMCF-BM or 08B1-1, Fodje *et al.*, 2014) at the Canadian Light Source (CLS). 08B1-1 is a bending magnet beamline with a Si (111) double crystal monochromator. Two-dimensional (2D) data were obtained using a Rayonix MX300HE detector with an active area of 300×300 mm^2. The patterns were collected at an energy of 18 keV ($\lambda = 0.688\,80$ Å) and a sample–detector distance of 250 mm.

The 2D PXRD patterns were calibrated and integrated using the GSASII software package (Toby and Von Dreele, 2013). The sample–detector distance, detector centering, and tilt were calibrated using a lanthanum hexaboride (LaB_6) standard reference material (NIST SRM 660a LaB6) and the calibration parameters were applied to all patterns. After calibration, the 2D patterns were integrated to obtain standard 1D powder diffraction patterns. A pattern collected from an empty Kapton capillary (using the same conditions) was subtracted from the sample data during integration.

Initial search/match phase identification performed with the Powder Diffraction File (ICDD, 2015) failed to find any suitable matches, although similar phases with significant lattice parameter differences were identified after *ab initio* indexing.

Pattern indexing with DICVOL06 (Boultif and Louer, 2004) suggested an orthorhombic unit cell with lattice parameters $a = 13.5570$, $b = 9.3063$, $c = 7.6188$ Å, and a cell volume of 961.22 Å^3 ($M_{20} = 50.9$, $F_{20} = 236.8$). Space-group determination with ChekCell (Laugier and Bochu, 2000) suggested space groups *Pnam* and $Pna2_1$ as equally plausible options. Subsequently, a reduced cell search of the Inorganic Crystal Structure Database (Hellenbrandt, 2004) using an unusually

[a]Author to whom correspondence should be addressed. Electronic mail: joel.reid@lightsource.ca

https://doi.org/10.1017/S0885715617000380 Published online by Cambridge University Press

large tolerance of 3% yielded the structure of diammonium trimolybdate, $(NH_4)_2Mo_3O_{10}$ (Range and Fässler, 1990), in space group *Pnma*.

Insufficient powder was available for an elemental analysis, but it was known that both sodium and ammonium were present during the processing. The *ab initio* lattice parameters were also reasonably similar to lattice parameters attributed to an orthorhombic trimolybdate phase observed by Förster *et al.* (1985), with formula $Na(NH_4)Mo_3O_{10}\cdot H_2O$ (lattice parameters $a = 9.25$, $b = 7.58$, and $c = 13.47$ Å). Therefore, a matrix was prepared for structure solution using the two space-group options with three cation compositions including: (1) two Na^{1+} ions, (2) two NH_4^{1+} ions, and (3) a mixed cation composition. Ammonium and MoO_6 fragments were converted to Fenske–Hall *Z*-matrices using Open Babel (O'Boyle *et al.*, 2011) and the full matrix of two space groups with three compositions was used to solve the structure using FOX (Favre-Nicolin and Černý, 2002). While the mixed cation compositions were clearly superior options, both space groups yielded comparable solutions and were examined in detail with Rietveld refinement. The *Pnma* structure was eventually chosen to be correct, based on similar agreement indices between structures with fewer parameter for *Pnma*, and by analogy with the diammonium trimolybdate structure (Range and Fässler, 1990).

Rietveld refinement of the crystal structure was performed with the GSAS/EXPGUI program (Toby, 2001; Larson and Von Dreele, 2004). Anomalous scattering factors were interpolated from the tables of Sasaki (1989) and input into GSAS. The background was refined using a Chebyshev polynomial with 12 terms. The positions of the Na, N, Mo, and O atoms were refined, while the positions of the ammonium H atoms remained fixed, but were periodically optimized using Avogadro (Hanwell *et al.*, 2012). Isotropic displacement parameters were refined for the Na, N, and Mo atoms, with the H atoms for the ammonium ion constrained to 1.3 times the value of the N atom. The isotropic displacement parameter for the O atoms refined to a fairly low value, a common issue in the presence of heavy atoms (Kaduk, 2007), but stayed positive with the use of the anomalous scattering factors. The position of the H atom for the water molecule was added late in the refinement based on the results of the density functional theory (DFT) calculation.

TABLE I. The crystal data, data collection and refinement parameters obtained for $Na(NH_4)Mo_3O_{10}\cdot H_2O$.

Crystal data, data collection, and refinement parameters	
Formula, *Z*	$Na(NH_4)Mo_3O_{10}\cdot H_2O$, $Z = 4$
Molecular mass (M_r)	506.91 g mol^{-1}
Symmetry, space group	Orthorhombic, *Pnma* (62)
Unit-cell parameters	$a = 13.549\,82(10)$, $b = 7.618\,50(6)$, $c = 9.302\,74(7)$ Å
Volume	960.32 (2) Å^3
Density (ρ_{calc})	3.506 g cm^{-3}
Beamline	CLS 08B1-1
Monochromator	Si (111) double crystal monochromator
Detector	Rayonix MX300HE (300 × 300 mm)
Specimen mounting	0.5 mm Kapton capillary
Collection mode	Transmission
Wavelength	$\lambda = 0.688\,80$ Å
Collection range, step size	2° to 39° (2θ), 0.005°/step
Number of data points	7400
Number of reflections	500
Background correction	12-term Chebyshev polynomial
Number of refined parameters	54
R_p	0.0338
R_{wp}	0.0469
R_{exp}	0.0371
χ^2	1.61

The crystal data, data collection, and refinement details are summarized in Table I.

A density functional geometry optimization (using a fixed experimental unit cell) was carried out using CRYSTAL14 (Dovesi *et al.*, 2014). The basis sets were obtained from the literature for the H, N, and O (Gatti *et al.*, 1994), Na (Dovesi *et al.*, 1991), and Mo atoms (Cora *et al.*, 1997). The calculation was run on eight 2.1 GHz Xeon cores (each with 6 Gb RAM) of a 304-core Dell Linux cluster at the Illinois

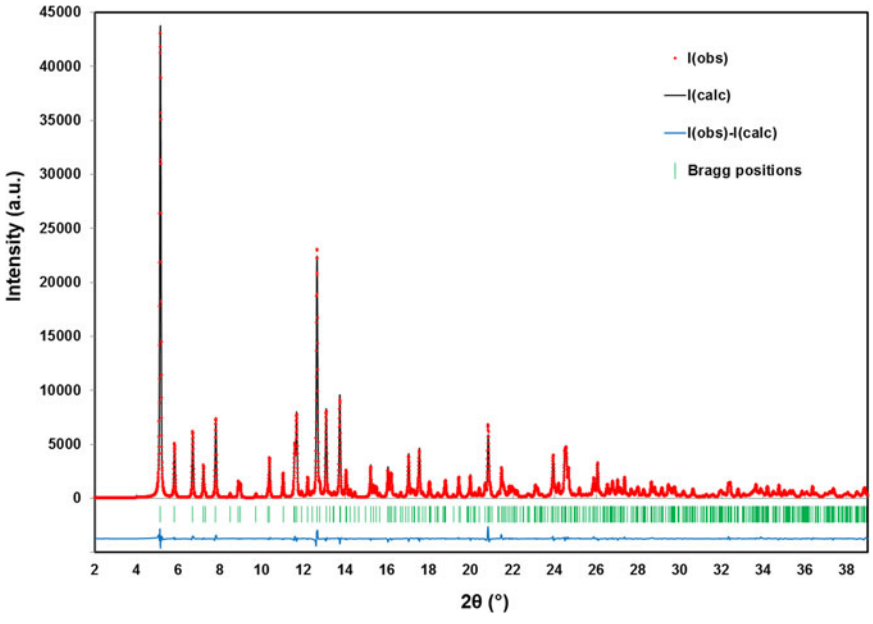


Figure 1. (Color online) A plot illustrating the final Rietveld refinement of $Na(NH_4)Mo_3O_{10}\cdot H_2O$ obtained with GSAS.

https://doi.org/10.1017/S0885715617000380 Published online by Cambridge University Press

TABLE II. The refined crystal structure of $Na(NH_4)Mo_3O_{10}\cdot H_2O$ with lattice parameters $a = 13.549\,82(10)$, $b = 7.618\,50(6)$, $c = 9.302\,74(7)$ Å. All atoms were refined with fixed site occupancies of 1.

Atom	*x/a*	*y/b*	*z/c*	Wyckoff	U_{iso} (Å^2)
Na1	0.311 19(23)	0.75	0.457 58(32)	4c	0.0151(11)
N2	0.6055(5)	0.75	0.4763(6)	4c	0.0232(19)
H3	0.666 11	0.75	0.540 46	4c	0.0302(24)
H4	0.571 41	0.636 07	0.503 22	8d	0.0302(24)
H5	0.639 73	0.75	0.379 18	4c	0.0302(24)
Mo6	0.596 25(6)	0.25	0.166 13(7)	4c	0.004 90(23)
Mo7	0.598 77(4)	0.496 95(7)	0.870 33(5)	8d	0.005 51(16)
O8	0.561 15(19)	0.4882(4)	0.108 20(34)	8d	0.0049(4)
O9	0.720 71(31)	0.25	0.1483(5)	4c	0.0049(4)
O10	0.433 16(30)	0.25	0.1308(6)	4c	0.0049(4)
O11	0.280 70(20)	0.4711(4)	0.087 12(29)	8d	0.0049(4)
O12	0.574 82(31)	0.25	0.3476(5)	4c	0.0049(4)
O13	0.585 26(34)	0.25	0.9212(5)	4c	0.0049(4)
O14	0.598 36(22)	0.4569(4)	0.687 88(29)	8d	0.0049(4)
O15	0.680 52(29)	0.75	1.2048(5)	4c	0.0049(4)
H16	0.640 73	0.647 94	1.172 26	8d	0.0063(5)

Institute of Technology (IIT), used 8 *k*-points and the B3LYP functional, and took approximately 1 day.

III. RESULTS AND DISCUSSION

Figure 1 illustrates the final Rietveld refinement of $Na(NH_4)Mo_3O_{10}\cdot H_2O$, which yielded a final reduced χ^2 of 1.61, while the refined atomic coordinates and DFT-optimized coordinates are given in Tables II and III, respectively. The root-mean square (RMS) Cartesian displacement between the Rietveld refined and DFT calculated structures for the heavy (non-hydrogen) atoms is 0.0415 Å, suggesting excellent agreement between refined and calculated structures. The largest peak and hole in the difference Fourier map were 0.357 and −0.395 *e* Å^{-3} respectively.

The refined lattice parameters [$a = 13.549\,82(10)$, $b = 7.618\,50(6)$, $c = 9.302\,74(7)$ Å] differ from the lattice parameters tabulated by Förster *et al.* (1985), yielding a 1.7% increase in the unit-cell volume. The cell volumes for two additional compounds tabulated by Förster *et al.* (1985), $K_2Mo_3O_{10}$ and $Cs_2Mo_3O_{10}$, were compared with independent analyses in the literature (by Seleborg, 1966; Enjalbert *et al.*, 1999, respectively). The independent analyses of $K_2Mo_3O_{10}$ and $Cs_2Mo_3O_{10}$ yielded unit-cell volume differences of −5.1 and +2.5%, respectively, relative to the cell volumes of Förster *et al.* (1985), suggesting the volume difference observed in this work is not unreasonable for the expected formula. An experimental pattern for $Na(NH_4)Mo_3O_{10}\cdot H_2O$ (PDF 00-036-0335, submitted by A. Förster, private communication) shows approximate agreement with the main reflection positions observed in this work, but has visually estimated intensities. A plot comparing the current data with PDF 00-036-0335 is contained in the online supplementary material.

TABLE III. The DFT optimized crystal structure of $Na(NH_4)Mo_3O_{10}\cdot H_2O$ calculated with fixed lattice parameters $a = 13.5527$, $b = 7.6203$, and $c = 9.3047$ Å.

Atom	*x/a*	*y/b*	*z/c*
Na1	0.311 30	0.75	0.457 27
N2	0.614 85	0.75	0.480 62
H3	0.674 75	0.75	0.550 51
H4	0.573 13	0.641 59	0.501 84
H5	0.641 55	0.75	0.373 94
Mo6	0.596 29	0.25	0.171 85
Mo7	0.600 97	0.496 94	0.867 88
O8	0.562 55	0.488 56	0.112 53
O9	0.723 04	0.25	0.156 84
O10	0.432 73	0.25	0.129 78
O11	0.277 33	0.468 55	0.087 12
O12	0.574 43	0.25	0.355 50
O13	0.587 65	0.25	0.922 89
O14	0.600 59	0.456 22	0.685 11
O15	0.678 36	0.75	1.203 22
H16	0.639 07	0.647 73	1.170 96

The crystal structure, illustrated in Figure 2, is characterized by molybdate ($Mo_3O_{10}^{2-}$) chains running parallel the *b*-axis, where adjacent molybdate octahedra share edges. The cations and water molecule provide linkages between the chains. Similar molybdate chains have been observed previously in a number of structures, with both orthorhombic and monoclinic symmetry ($P2_1/m$), including $(NH_4)_2Mo_3O_{10}$ (Range and Fässler, 1990), $Na(NH_4)Mo_3O_{10}$ (Xu *et al.*, 1996) and $(NH_4)_2Mo_3O_{10}\cdot H_2O$ (Lasocha *et al.*, 1995). The MoO_6 octahedra observed in the previous studies have generally been distorted, and the current structure is no exception; the Rietveld refined Mo–O bond lengths cover a range of nearly 0.6 Å for each Mo atom, as summarized in Table IV. In terms of both range and limits, these values are consistent with previous single-crystal observations (Range and Fässler, 1990; Xu *et al.*, 1996), although Lasocha *et al.* (1995) observed two larger Mo–O distances of 2.50 and 2.62 Å using powder data. The bond valence sum (BVS) values (Brown, 2002) are given in Table V. Despite the distortion of the MoO_6 octahedra, the BVS values for the Mo atoms are very close to the expected values [6.013(32) for Mo6, 5.974 (19) for Mo7]. The BVS value for the Na ion [1.218(6)], which is six-coordinate, is somewhat larger than the value for the ammonium ion [0.855(6)], but comparable with the BVS value for Na [1.193(1)] observed in the similar compound $Na(NH_4)Mo_3O_{10}$ (Xu *et al.*, 1996). While the

https://doi.org/10.1017/S0885715617000380 Published online by Cambridge University Press

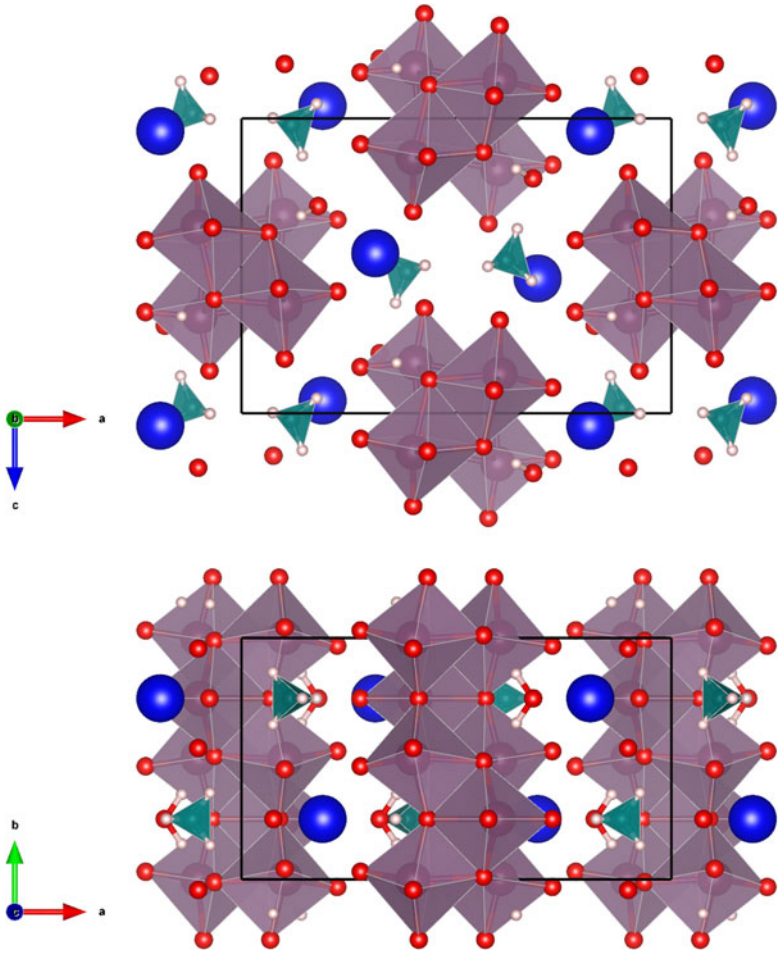


Figure 2. (Color online) The crystal structure of $Na(NH_4)Mo_3O_{10}\cdot H_2O$, viewed along the *b*-axis (top) and *c*-axis (bottom). The polyhedra and atom types can be identified by color including NH_4 (green tetrahedra), MoO_6 (purple octahedra), Na (dark blue), hydrogen (pink), and O (red). The unit cell is outlined in black. The figure was prepared with VESTA (Momma and Izumi, 2011).

TABLE IV. Mo–O bond lengths obtained from the Rietveld refinement and DFT calculation.

Bond	Rietveld (Å)	DFT (Å)	Bond	Rietveld (Å)	DFT (Å)
Mo6–O8	1.952 (3)	1.954	Mo7–O8	2.272 (3)	2.336
Mo6–O8	1.952 (3)	1.954	Mo7–O8	2.179 (3)	2.226
Mo6–O9	1.695 (4)	1.723	Mo7–O10	1.976 (1)	1.982
Mo6–O10	2.234 (4)	2.251	Mo7–O11	1.698 (3)	1.722
Mo6–O12	1.713 (5)	1.734	Mo7–O13	1.949 (1)	1.958
Mo6–O13	2.283 (4)	2.319	Mo7–O14	1.724 (3)	1.729

TABLE V. Some bond valence parameters calculated from the refined $Na(NH_4)Mo_3O_{10}\cdot H_2O$ structure, using a maximum bond distance of 3 Å.

Atom	Valence	Bond valence sum
Na1	+1	1.218(6)
NH_4	+1	0.855(6)
Mo6	+6	6.013(32)
Mo7	+6	5.974(19)
O8	−2	2.022(9)
O9	−2	1.966(20)
O10	−2	2.074(5)
O11	−2	1.997(13)
O12	−2	2.043(23)
O13	−2	2.149(6)
O14	−2	1.962(12)
O15	−2	1.973(11)
H16	+1	1.066(7)

ammonium ion BVS value is low, if two oxygen bonds at 3.24 Å are included (above the current calculation limit of 3 Å), the BVS value increases to 0.984(7).

Hydrogen bonding in the structure, based on the DFT model, is summarized in Table VI. The short bonds Mo6–O9, Mo6–O12, Mo7–O11 and Mo7–O14 are double bonds, and with the exception of the water molecule, O15, all of the hydrogen bonds involve these O atoms as acceptors. The ammonium ion forms discrete N–H...O bonds between two adjacent chains (via O9 in one chain, via O12 and O14 in the second chain) in addition to a fourth bond with the water O15, itself hydrogen bonded to a third chain. The water molecule forms two hydrogen bonds within a single chain, where the O–H...O hydrogen bonds form a R1,1(6) ring, which includes both a Mo and the Na. The hydrogen bonds also participate in a number of more-complex rings and chains.

A Bragg reflection list, shown in Table VII, was prepared by summing reflections closer than 0.02°2θ as multiple reflections and assigning a weighted average reflection position, then including all reflections with relative integrated intensities of 0.3% or greater up to 30°2θ. The Bragg reflection list and raw data are contained in a crystallographic information file (CIF) in the online supplementary material. Individual CIF files containing the Rietveld refined and DFT calculated structures are also included as online supplementary material.

https://doi.org/10.1017/S0885715617000380 Published online by Cambridge University Press

TABLE VI. Hydrogen bonds observed in the $Na(NH_4)Mo_3O_{10}\cdot H_2O$ structure and their parameters as determined by the DFT modeling.

H-bond	D–H (Å)	H...A (Å)	D...A (Å)	D–H...A (°)	Overlap (*e*)	E (kcal mol^{-1})
O15–H16...O8	0.990	1.686	2.673	174.0	0.047	11.8
N2–H5...O15	1.057	1.665	2.721	177.4	0.107	
N2–H4...O14	1.020	2.245	2.944	124.4	0.017	
N2–H4...O12	1.020	2.539	2.984	105.9	0.008	
N2–H3...O9	1.040	1.702	2.741	176.8	0.063	

TABLE VII. The Bragg reflection list obtained from the final Rietveld refinement, prepared by summing reflections closer than 0.02 °2θ as multiple reflections and assigning a weighted average reflection position, then including all reflections with relative integrated intensities of 0.3% or greater up to 30 °2θ.

h	*k*	*l*	d_{calc} (Å)	d_{obs} (Å)	$2\theta_{calc}$ (°)	$2\theta_{obs}$ (°)	I/I_{max} (%)	$\Delta 2\theta$ (°)
1	0	1	7.669 22	7.668 73	5.148	5.148	100.0	0.000
2	0	0	6.774 91	6.774 60	5.828	5.828	11.4	0.000
0	1	1	5.894 17	5.894 58	6.699	6.699	13.7	0.000
2	0	1	5.476 51	5.476 55	7.211	7.211	6.8	0.000
1	1	1	5.404 94	5.404 69	7.307	7.307	0.9	0.000
2	1	0	5.062 67	5.062 92	7.801	7.801	16.4	0.000
0	0	2	4.651 37	4.651 61	8.492	8.492	0.9	0.000
2	1	1	4.446 82	4.446 75	8.884	8.884	3.5	0.000
1	0	2	4.399 37	4.399 31	8.980	8.980	3.0	0.000
3	0	1	4.063 04	4.063 01	9.725	9.725	0.9	0.000
2	0	2	3.834 61	3.834 52	10.306	10.306	0.9	0.000
1	1	2	3.809 79	3.809 82	10.373	10.373	8.5	0.000
0	2	0	3.809 25	3.809 82	10.375	10.373	8.5	0.002
3	1	1	3.585 07	3.585 15	11.025	11.025	5.3	0.000
2	1	2	3.425 21	3.425 07	11.542	11.542	1.6	0.000
1	2	1	3.411 60	3.411 52	11.588	11.588	9.7	0.000
4	0	0	3.387 46	3.387 34	11.671	11.671	17.5	0.000
2	2	0	3.320 39	3.320 44	11.907	11.907	1.1	0.000
3	0	2	3.240 32	3.240 19	12.203	12.203	4.3	0.000
4	0	1	3.183 00	3.183 03	12.423	12.423	0.8	0.000
2	2	1	3.127 17	3.127 12	12.646	12.646	52.6	0.000
4	1	0	3.095 28	3.095 19	12.777	12.777	2.0	0.000
1	0	3	3.022 77	3.022 87	13.084	13.084	18.9	0.000
3	1	2	2.981 82	2.981 80	13.265	13.265	0.8	0.000
4	1	1	2.936 97	2.937 06	13.468	13.468	0.9	0.000
1	2	2	2.879 76	2.879 82	13.737	13.737	22.0	0.000
2	0	3	2.819 60	2.819 57	14.032	14.032	5.5	0.000
1	1	3	2.809 69	2.809 60	14.082	14.082	1.4	0.000
3	2	1	2.778 94	2.778 98	14.238	14.238	1.6	0.000
4	0	2	2.738 26	2.738 23	14.451	14.451	1.1	0.000
5	0	1	2.601 82	2.601 82	15.213	15.213	6.9	0.000
4	1	2	2.576 87	2.576 90	15.361	15.361	2.6	0.000
3	0	3	2.556 41	2.556 39	15.485	15.485	2.3	0.000
4	2	0	2.531 34	2.531 37	15.639	15.639	0.8	0.000
3	2	2	2.468 14	2.468 18	16.042	16.042	6.2	0.000
0	3	1	2.449 86	2.449 82	16.163	16.163	2.7	0.000
4	2	1	2.442 53	2.442 47	16.212	16.212	4.5	0.000
3	1	3	2.423 60	2.423 61	16.339	16.339	0.3	0.000
1	3	1	2.410 77	2.410 72	16.427	16.427	0.5	0.000
2	3	0	2.377 93	2.377 94	16.655	16.655	1.1	0.000
0	0	4	2.325 69	2.325 68	17.032	17.032	9.6	0.000
2	3	1	2.303 86	2.303 80	17.195	17.195	1.4	0.000
1	0	4	2.292 17	2.292 16	17.283	17.283	1.5	0.000
2	2	3	2.266 30	2.266 27	17.482	17.482	1.6	0.000
6	0	0	2.258 30	2.258 32	17.544	17.544	10.7	0.000
5	1	2	2.238 21	2.238 19	17.703	17.703	1.0	0.000
2	0	4	2.199 69	2.199 62	18.015	18.016	2.7	−0.001
1	3	2	2.199 38	2.199 62	18.018	18.016	2.7	0.002
1	1	4	2.194 97	2.194 79	18.054	18.056	1.9	−0.002
6	0	1	2.194 57	2.194 79	18.058	18.056	1.9	0.002
3	3	1	2.153 47	2.153 52	18.405	18.405	0.5	0.000
5	2	1	2.148 48	2.148 43	18.449	18.449	0.8	0.000

Continued

https://doi.org/10.1017/S0885715617000380 Published online by Cambridge University Press

TABLE VII. Continued

h	k	l	d_{calc} (Å)	d_{obs} (Å)	$2\theta_{calc}$ (°)	$2\theta_{obs}$ (°)	I/I_{max} (%)	$\Delta 2\theta$ (°)
3	2	3	2.122 70	2.122 65	18.675	18.675	0.3	0.000
2	1	4	2.113 36	2.113 35	18.758	18.758	1.3	0.000
6	1	1	2.108 82	2.108 78	18.799	18.799	3.4	0.000
3	0	4	2.067 67	2.067 70	19.176	19.176	0.6	0.000
5	0	3	2.040 54	2.040 50	19.434	19.434	4.7	0.000
6	0	2	2.031 52	2.031 50	19.521	19.521	0.4	0.000
4	3	1	1.985 11	1.984 99	19.982	19.983	5.1	−0.001
0	2	4	1.984 97	1.984 99	19.983	19.983	5.1	0.000
1	2	4	1.964 01	1.963 40	20.199	20.205	0.9	−0.006
6	1	2	1.962 93	1.963 40	20.210	20.205	0.9	0.005
1	3	3	1.944 39	1.943 32	20.405	20.416	2.1	−0.011
6	2	0	1.942 58	1.943 32	20.424	20.416	2.1	0.008
4	0	4	1.917 30	1.917 31	20.696	20.696	2.9	0.000
2	2	4	1.904 90	1.904 66	20.832	20.835	13.3	−0.003
0	4	0	1.904 63	1.904 66	20.835	20.835	13.3	0.000
6	2	1	1.901 57	1.901 59	20.869	20.869	3.2	0.000
7	0	1	1.895 10	1.895 13	20.941	20.941	1.6	0.000
4	3	2	1.862 00	1.861 99	21.318	21.318	0.7	0.000
4	1	4	1.859 33	1.859 32	21.349	21.349	0.4	0.000
1	4	1	1.848 47	1.848 45	21.476	21.476	6.2	0.000
1	0	5	1.843 25	1.843 28	21.537	21.537	1.8	0.000
7	1	1	1.839 06	1.839 06	21.587	21.587	1.5	0.000
2	4	0	1.833 55	1.833 52	21.653	21.653	0.8	0.000
3	2	4	1.817 22	1.817 19	21.850	21.850	2.5	0.000
0	1	5	1.807 43	1.807 46	21.969	21.969	2.4	0.000
3	3	3	1.801 65	1.801 63	22.041	22.041	0.5	0.000
2	4	1	1.798 94	1.798 81	22.074	22.076	1.2	−0.002
5	2	3	1.798 72	1.798 81	22.077	22.076	1.2	0.001
7	0	2	1.787 11	1.787 14	22.222	22.222	1.5	0.000
1	4	2	1.747 86	1.747 63	22.728	22.731	0.6	−0.003
2	1	5	1.746 35	1.747 63	22.748	22.731	0.6	0.017
7	1	2	1.739 89	1.739 92	22.834	22.833	0.5	0.001
5	3	2	1.721 45	1.721 48	23.081	23.081	0.6	0.000
5	1	4	1.719 34	1.719 35	23.110	23.110	2.2	0.000
4	2	4	1.712 60	1.712 62	23.202	23.202	1.9	0.000
1	3	4	1.701 55	1.701 56	23.355	23.355	0.3	0.000
7	2	1	1.696 72	1.696 69	23.423	23.423	0.4	0.000
8	0	1	1.666 33	1.666 33	23.856	23.856	0.6	0.000
2	3	4	1.662 67	1.662 69	23.909	23.909	0.3	0.000
4	4	0	1.660 20	1.659 81	23.945	23.951	10.0	−0.006
1	2	5	1.659 21	1.659 81	23.960	23.951	10.0	0.009
8	1	0	1.653 36	1.653 35	24.046	24.046	1.3	0.000
6	2	3	1.646 23	1.646 20	24.152	24.152	0.8	0.000
7	0	3	1.642 03	1.641 98	24.214	24.215	2.8	−0.001
3	4	2	1.641 98	1.641 98	24.215	24.215	2.8	0.000
4	0	5	1.630 76	1.630 77	24.384	24.384	0.4	0.000
2	2	5	1.623 10	1.623 10	24.501	24.501	8.5	0.000
6	0	4	1.620 16	1.620 17	24.546	24.546	4.8	0.000
7	2	2	1.617 91	1.617 90	24.581	24.581	7.1	0.000
1	4	3	1.611 42	1.611 45	24.681	24.681	6.2	0.000
7	1	3	1.605 17	1.605 17	24.779	24.779	0.7	0.000
4	1	5	1.594 64	1.594 66	24.945	24.945	0.5	0.000
2	4	3	1.578 28	1.578 29	25.208	25.208	2.1	0.000
3	2	5	1.567 84	1.567 83	25.379	25.379	0.4	0.000
4	4	2	1.563 58	1.563 58	25.449	25.449	0.3	0.000
8	1	2	1.557 87	1.557 86	25.544	25.544	0.5	0.000
0	0	6	1.550 46	1.550 46	25.668	25.668	0.5	0.000
8	2	0	1.547 64	1.547 62	25.716	25.716	0.3	0.000
1	0	6	1.540 40	1.540 38	25.838	25.839	1.2	−0.001
5	4	1	1.536 85	1.536 87	25.899	25.899	3.8	0.000
5	0	5	1.533 84	1.533 84	25.951	25.951	0.7	0.000
3	4	3	1.527 33	1.526 73	26.064	26.074	8.1	−0.010
8	2	1	1.526 66	1.526 73	26.075	26.074	8.1	0.001
7	3	1	1.518 81	1.518 83	26.212	26.212	0.9	0.000
0	5	1	1.503 66	1.503 67	26.481	26.481	0.3	0.000
0	3	5	1.500 85	1.500 84	26.532	26.532	1.7	0.000

Continued

https://doi.org/10.1017/S0885715617000380 Published online by Cambridge University Press

TABLE VII. Continued

h	k	l	d_{calc} (Å)	d_{obs} (Å)	$2\theta_{calc}$ (°)	$2\theta_{obs}$ (°)	I/I_{max} (%)	$\Delta 2\theta$ (°)
4	2	5	1.499 16	1.499 17	26.562	26.562	1.8	0.000
6	2	4	1.490 91	1.490 90	26.712	26.712	1.0	0.000
7	0	4	1.487 79	1.487 79	26.769	26.769	0.6	0.000
8	0	3	1.486 45	1.486 37	26.794	26.795	3.0	−0.001
9	0	1	1.486 20	1.486 37	26.798	26.795	3.0	0.003
2	1	6	1.482 49	1.482 51	26.866	26.866	0.7	0.000
0	4	4	1.473 54	1.473 52	27.033	27.033	4.1	0.000
3	0	6	1.466 46	1.466 45	27.166	27.166	1.6	0.000
1	4	4	1.464 90	1.464 91	27.195	27.195	0.3	0.000
6	4	0	1.455 95	1.455 93	27.366	27.366	4.5	0.000
5	3	4	1.449 26	1.449 28	27.494	27.494	0.6	0.000
2	4	4	1.439 88	1.439 83	27.677	27.678	1.6	−0.001
1	5	2	1.439 79	1.439 83	27.679	27.678	1.6	0.001
6	4	1	1.438 44	1.438 46	27.705	27.705	0.3	0.000
0	2	6	1.436 06	1.436 02	27.752	27.753	0.9	−0.001
6	0	5	1.435 97	1.436 02	27.754	27.753	0.9	0.001
1	2	6	1.428 06	1.428 05	27.911	27.911	0.7	0.000
3	5	1	1.426 68	1.426 70	27.938	27.938	0.5	0.000
3	3	5	1.424 27	1.424 25	27.986	27.987	0.7	−0.001
5	2	5	1.422 83	1.422 85	28.016	28.015	1.8	0.001
6	1	5	1.411 13	1.411 11	28.253	28.253	0.7	0.000
4	0	6	1.409 80	1.409 50	28.280	28.286	1.2	−0.006
8	3	0	1.409 08	1.409 50	28.295	28.286	1.2	0.009
9	1	2	1.407 71	1.407 69	28.323	28.323	0.4	0.000
5	4	3	1.392 35	1.392 34	28.642	28.642	3.4	0.000
4	5	0	1.389 60	1.389 53	28.700	28.701	0.7	−0.001
6	4	2	1.389 47	1.389 53	28.702	28.701	0.7	0.001
4	1	6	1.386 27	1.385 99	28.770	28.776	0.7	−0.006
7	2	4	1.385 83	1.385 99	28.779	28.776	0.7	0.003
8	2	3	1.384 75	1.384 72	28.802	28.803	1.8	−0.001
9	2	1	1.384 55	1.384 72	28.807	28.803	1.8	0.004
7	3	3	1.378 89	1.378 91	28.927	28.927	0.7	0.000
3	5	2	1.378 86	1.378 91	28.928	28.927	0.7	0.001
4	3	5	1.372 20	1.372 22	29.072	29.071	0.4	0.001
3	2	6	1.368 55	1.368 54	29.151	29.151	2.2	0.000
10	0	0	1.354 98	1.354 81	29.449	29.453	2.8	−0.004
9	0	3	1.354 35	1.354 81	29.463	29.453	2.8	0.010
4	4	4	1.351 23	1.351 22	29.533	29.533	2.1	0.000
8	1	4	1.347 54	1.347 52	29.616	29.616	0.4	−0.001
6	2	5	1.343 67	1.343 53	29.703	29.706	1.8	−0.003
7	4	1	1.343 39	1.343 53	29.709	29.706	1.8	0.003
7	0	5	1.341 38	1.340 79	29.755	29.768	2.0	−0.013
9	2	2	1.340 72	1.340 79	29.770	29.768	2.0	0.002
4	5	2	1.331 45	1.331 44	29.982	29.982	0.3	0.000

SUPPLEMENTARY MATERIAL

The supplementary material for this article can be found at https://doi.org/10.1017/S0885715617000380.

ACKNOWLEDGEMENTS

The authors thank Andrey Rogachev for the use of the computing resources at the Illinois Institute of Technology, and suggestions from two anonymous reviewers which significantly improved the manuscript. This paper is dedicated to Professor Emeritus Michael Sayer (Queen's University) and his enthusiasm for all things physics, chemistry, materials science and beyond. Research described in this paper was performed using beamline 08B1-1 at the Canadian Light Source, which is supported by the Canadian Foundation for Innovation, the Natural Sciences and Engineering Research Council of Canada, the National Research Council Canada, the Canadian Institutes of Health Research, the Government of Saskatchewan, Western Economic Diversification Canada, and the University of Saskatchewan.

Anbar, A. D. (**2004**). "Molybdenum stable isotopes: observation, interpretations and directions," Rev. Mineral. Geochem. **55**, 429–454.

Banerjee, S., Pillai, M. R. A., and Ramamoorthy, N. (**2001**). "Evolution of Tc-99 m in diagnostic radiopharmaceuticals," Sem. Nucl. Med. **31**, 260–277.

Boultif, A. and Louer, D. (**2004**). "Powder pattern indexing with the dichotomy method," J. Appl. Crystallogr. **37**, 724–731.

Brown, I. D. (**2002**). *The Chemical Bond in Inorganic Chemistry: The Bond Valence Model* (Oxford University Press, New York).

Chippendale, A. M. and Cheetham, A. K. (**1994**). "The Oxide Chemistry of Molybdenum," in *Molybdenum: An Outline of its Chemistry and Uses*, edited by E. R. Braithwaite and J. Haber (Elsevier, Amsterdam), pp. 146–184.

Cora, F., Patel, A., Harrison, N. M., Roetti, C., and Catlow, C. R. A. (**1997**). "An ab-initio Hartree-Fock study of alpha-MoO3," J. Mater. Chem. **7**, 959–967.

https://doi.org/10.1017/S0885715617000380 Published online by Cambridge University Press

Dovesi, R., Roetti, C., Freyria Fava, C., Prencipe, M., and Saunders, V. R. (**1991**). "On the elastic properties of lithium, sodium and potassium oxide. An ab initio study," Chem. Phys. **156**, 11–19.

Dovesi, R., Orlando, R., Erba, A., Zicovich-Wilson, C. M., Civalleri, B., Casassa, S., Maschio, L., Ferrabone, M., De La Pierre, M., D'Arco, P., Noel, Y., Causa, M., Rerat, M., and Kirtman, B. (**2014**). "CRYSTAL14: a program for the *Ab Initio* investigation of crystalline solids," Int. J. Quantum Chem. **114**, 1287–1313.

Enjalbert, R., Guinneton, F., and Galy, J. (**1999**). "$Cs_2Mo_3O_{10}$," Acta Crystallogr. **C55**, 273–276.

Favre-Nicolin, V. and Černý, R. (**2002**). "FOX, 'Free Objects for crystallography': a modular approach to *ab initio* structure determination from powder diffraction," J. Appl. Crystallogr. **35**, 734–743.

Fodje, M., Grochulski, P., Janzen, K., Labiuk, S., Gorin, J., and Berg, R. (**2014**). "08B1-1: an automated beamline for macromolecular crystallography experiments at the Canadian Light Source," J. Synchrotron Rad. **21**, 633–637.

Förster, A., Kreusler, H. U., and Fuchs, J. (**1985**). "Die kristallinen Phasen der Alkalitrimolybdate," Z. Naturforsch. **40b**, 1139–1148.

Garner, C. D. (**1994**). "The Chemical Nature of the Molybdenum Centres in Enzymes," in *Molybdenum: An Outline of its Chemistry and Uses*, edited by E. R. Braithwaite and J. Haber (Elsevier, Amsterdam), pp. 403–418.

Gatti, C., Saunders, V. R., and Roetti, C. (**1994**). "Crystal-field effects on the topological properties of the electron-density in molecular crystals – the case of urea," J. Chem. Phys. **101**, 10686–10696.

Green, M. L. H. (**1994**). "An Introduction to the Chemistry of Molybdenum," in *Molybdenum: An Outline of its Chemistry and Uses*, edited by E. R. Braithwaite and J. Haber (Elsevier, Amsterdam), pp. 95–145.

Haber, J. (**1994**). "Molybdenum Compounds in Heterogeneous Catalysis," in *Molybdenum: An Outline of its Chemistry and Uses*, edited by E. R. Braithwaite and J. Haber (Elsevier, Amsterdam), pp. 477–617.

Hanwell, M. D., Curtis, D. E., Lonie, D. C., Vandermeersch, T., Zurek, E., and Hutchison, G. R. (**2012**). "Avogadro: an advanced semantic chemical editor, visualization, and analysis platform," J. Cheminform. **4**, 17.

Hellenbrandt, M. (**2004**). "The inorganic crystal structure database (ICSD) – present and future," Crystallogr. Rev. **10**, 17–22.

ICDD (**2015**). PDF-4+ 2015 (Database), edited by Dr. Soorya Kabekkodu, International Centre for Diffraction Data, Newtown Square, PA, USA.

Kaduk, J. A. (**2007**). "Chemical reasonableness in Rietveld analysis: inorganics," Powder Diffr. **22**, 268–278.

Larson, A. C. and Von Dreele, R. B. (**2004**). *General Structure Analysis System (GSAS)* (Report No. LAUR 86-748). Los Alamos, NM: Los Alamos National Laboratory.

Lasheen, T. A., El-Almady, M. E., Haasib, H. B., and Helal, A. S. (**2015**). "Molybdenum metallurgy review: hydrometallurgical routes to recovery of molybdenum from ores and mineral raw materials," Miner. Proc. Extract. Metall. Rev. **36**, 145–173.

Lasocha, W., Jansen, J., and Schenk, H. (**1995**). "Crystal structure of ammonium trimolybdate monohydrate $(NH_4)_2Mo_3O_{10}\cdot H_2O$ by powder diffraction method," J. Solid State Chem. **116**, 422–426.

Laugier, J. and Bochu, B. (**2000**). "LMGP-Suite Suite of Programs for the interpretation of X-ray Experiments," ENSP/Laboratoire des Matériaux et du Génie Physique, BP 46. 38042 Saint Martin d'Hères, France. http://www.inpg.fr/LMGP and http://www.ccp14.ac.uk/tutorial/lmgp/

Momma, K., and Izumi, F. (**2011**). "VESTA 3 for three-dimensional visualization of crystal, volumetric and morphology data," J. Appl. Crystallogr. **44**, 1272–1276.

National Research Council (**2009**). *Medical Isotope Production Without Highly Enriched Uranium* (National Academies Press, Washington).

O'Boyle, N., Banck, M., James, C. A., Morley, C., Vandermeersch, T., and Hutchison, G. R. (**2011**). "Open babel: an open chemical toolbox," J. Chem. Inf., 1–14. doi: 10.1186/1758-2946-3-33.

Range, K.-J. and Fässler, A. (**1990**). "Diammonium trimolybdate(VI), $(NH4)_2Mo_3O_{10}$," Acta Crystallogr. **C46**, 488–489.

Roggan, S. and Limberg, C. (**2006**). "Molecular molybdenum/bismuth compounds," Inorg. Chim. Acta **359**, 4698–4722.

Sasaki, S. (**1989**). *Numerical Tables of Anomalous Scattering Factors Calculated by the Cromer and Lieberman's Method* (KEK Report 88-14).

Schwarz, G., Mendel, R. R., and Ribbe, M. W. (**2009**). "Molybdenum cofactors, enzymes and pathways," Nature **460**, 839–847.

Seleborg, M. (**1966**). "The crystal structure of dipotassium trimolybdate," Acta Chem. Scand. **20**, 2195–2201.

Sławiński, W. A., Fjellvåg, Ø., Ruud, A., and Fjellvåg, H. (**2016**). "A novel polytype – the stacking fault based γ-MoO_3 nanobelts," Acta Cryst. **B72**, 201–208.

Tkac, P. and Vandergrift, G. F. (**2016**). "Recycling of enriched Mo targets for economic production of $^{99}Mo/^{99m}Tc$ medical isotope without use of enriched uranium," J. Radioanal. Nucl. Chem. **308**, 205–212.

Toby, B. H. (**2001**). "EXPGUI, a graphical user interface for GSAS," J. Appl. Crystallogr. **34**, 210–213.

Toby, B. H. and Von Dreele, R. B. (**2013**). "GSAS II: the genesis of a modern open-source all-purpose crystallography software package," J. Appl. Crystallogr. **46**, 544–549.

Van Noorden, R. (**2013**). "The medical testing crisis," Nature **504**, 202–204.

Xu, Y., An, L. H., and Koh, L. L. (**1996**). "Investigations into the engineering of inorganic/organic solids: hydrothermal synthesis and structure characterization of one-dimensional molybdenum oxide polymers," Chem. Mater. **8**, 814–818.

Zaman, S. and Smith, K. J. (**2012**). "A review of molybdenum catalysts for synthesis gas conversion to alcohols: catalysts, mechanisms and kinetics," Catal. Rev. Sci. Eng. **54**, 41–132.

https://doi.org/10.1017/S0885715617000380 Published online by Cambridge University Press